Science Advances
AAAS

Supplementary Materials for

The prevalence and specificity of local protein synthesis during neuronal synaptic plasticity

Chao Sun, Andreas Nold, Claudia M. Fusco, Vidhya Rangaraju, Tatjana Tchumatchenko, Mike Heilemann, Erin M. Schuman*

*Corresponding author. Email: erin.schuman@brain.mpg.de

Published 17 September 2021, *Sci. Adv.* **7**, eabj0790 (2021)
DOI: 10.1126/sciadv.abj0790

This PDF file includes:

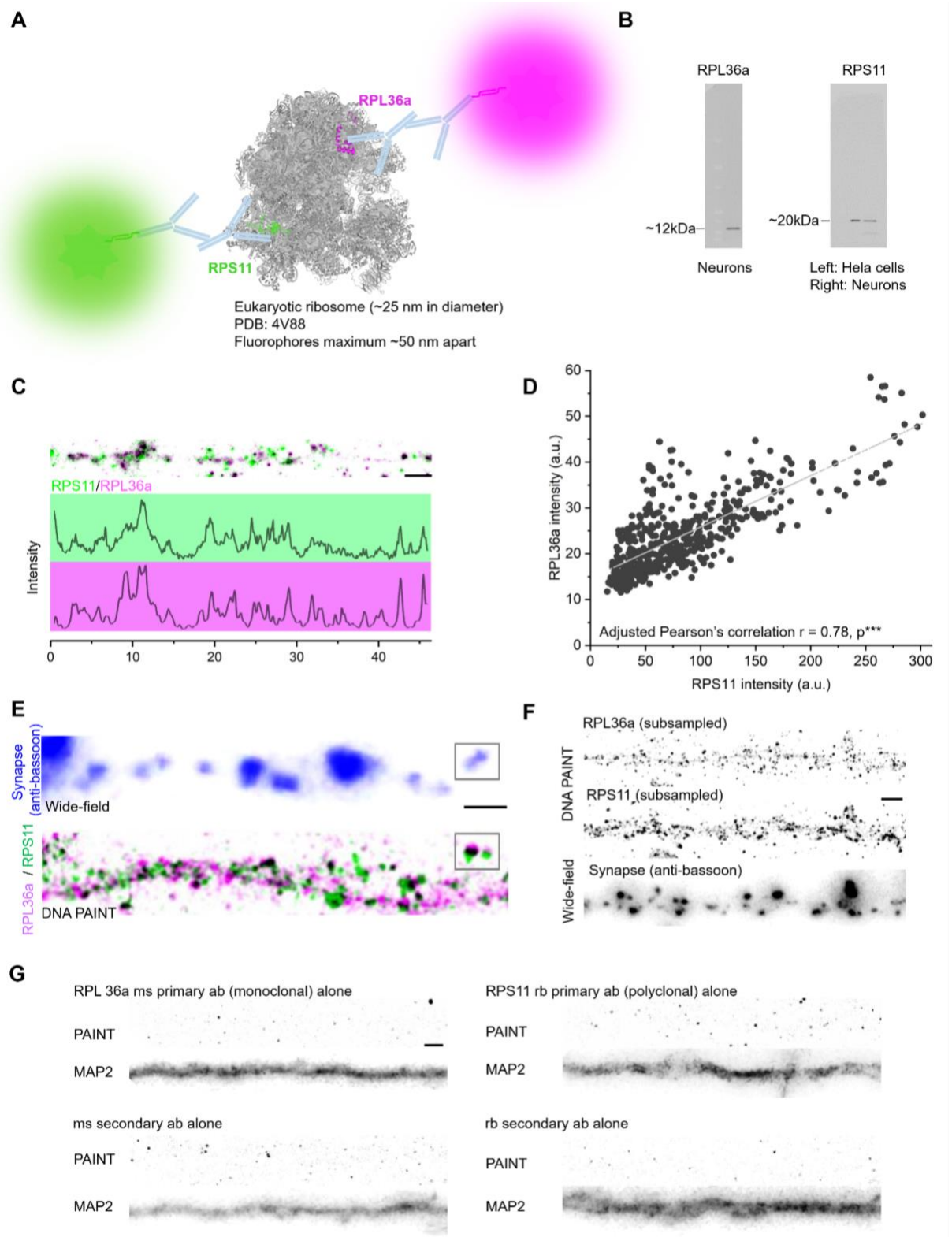
A
RPL36a
RPS11
Eukaryotic ribosome (~25 nm in diameter)
PDB: 4V88
Fluorophores maximum ~50 nm apart
B
RPL36a
RPS11
~12kDa
~20kDa
Neurons
Left: Hela cells
Right: Neurons
C
RPS11/RPL36a
Intensity
0
10
20
30
40
D
RPL36a intensity (a.u.)
RPS11 intensity (a.u.)
Adjusted Pearson's correlation r = 0.78, p***
0
50
100
150
200
250
300
10
20
30
40
50
60
E
Synapse (anti-bassoon)
Wide-field
RPL36a / RPS11
DNA PAINT
F
RPL36a (subsampled)
RPS11 (subsampled)
DNA PAINT
Synapse (anti-bassoon)
Wide-field
G
RPL 36a ms primary ab (monoclonal) alone
PAINT
MAP2
RPS11 rb primary ab (polyclonal) alone
PAINT
MAP2
ms secondary ab alone
PAINT
MAP2
rb secondary ab alone
PAINT
MAP2

Fig. S1.

Immunolabeling of ribosomal large- and small- subunits for multiplexed single-molecule localization of assembled ribosomes. (A) Scheme illustrating the labeling of ribosomal proteins RPL36a and RPS11 using primary and secondary antibodies to identify assembled ribosomes through coincidence detection. The scheme indicates that the fluorophores likely have a maximal separation of ~50nm due to the dimensions of ribosomes and the antibodies. **(B)** Rabbit, polyclonal, anti-RPS11 and mouse, monoclonal, anti-RPL36a antibodies were validated by western blot and exhibited a single band each, corresponding to the correct sizes of their epitopes, in Hela or neuronal cell lysates. **(C)** An example dendritic segment showing the colocalization of RPS11 (green) and RPL36a (magenta) labelling in a cultured rat hippocampal neuron. Bottom traces of corresponding colors show the pixel intensity profiles. Scale bar: 1 µm. **(D)** Scatter plot showing the significant, positive correlations between the pixel intensities of RPS11 and RPL36a in dendrites (Pearson's correlation r = 0.78, p***<0.001 with one tailed test). **(E)** An example dendritic segment (synapses visualized by guinea pig anti-bassoon immunostaining) showing the signal crowding of RPS11 (green) and RPL36a (magenta) localizations using DNA PAINT (See Methods). Scale bar: 1 µm. **(F)** An example dendritic segment demonstrating optimized signal abundance via reduced labeling of RPS11 and RPL36a *in situ*. Scale bar: 1 µm. **(G)** Example dendritic segments (indicated by MAP2 staining) showing the lack of RPS11 or RPL36a localizations in primary or secondary antibody leave-out, negative controls. Scale bar: 1 µm

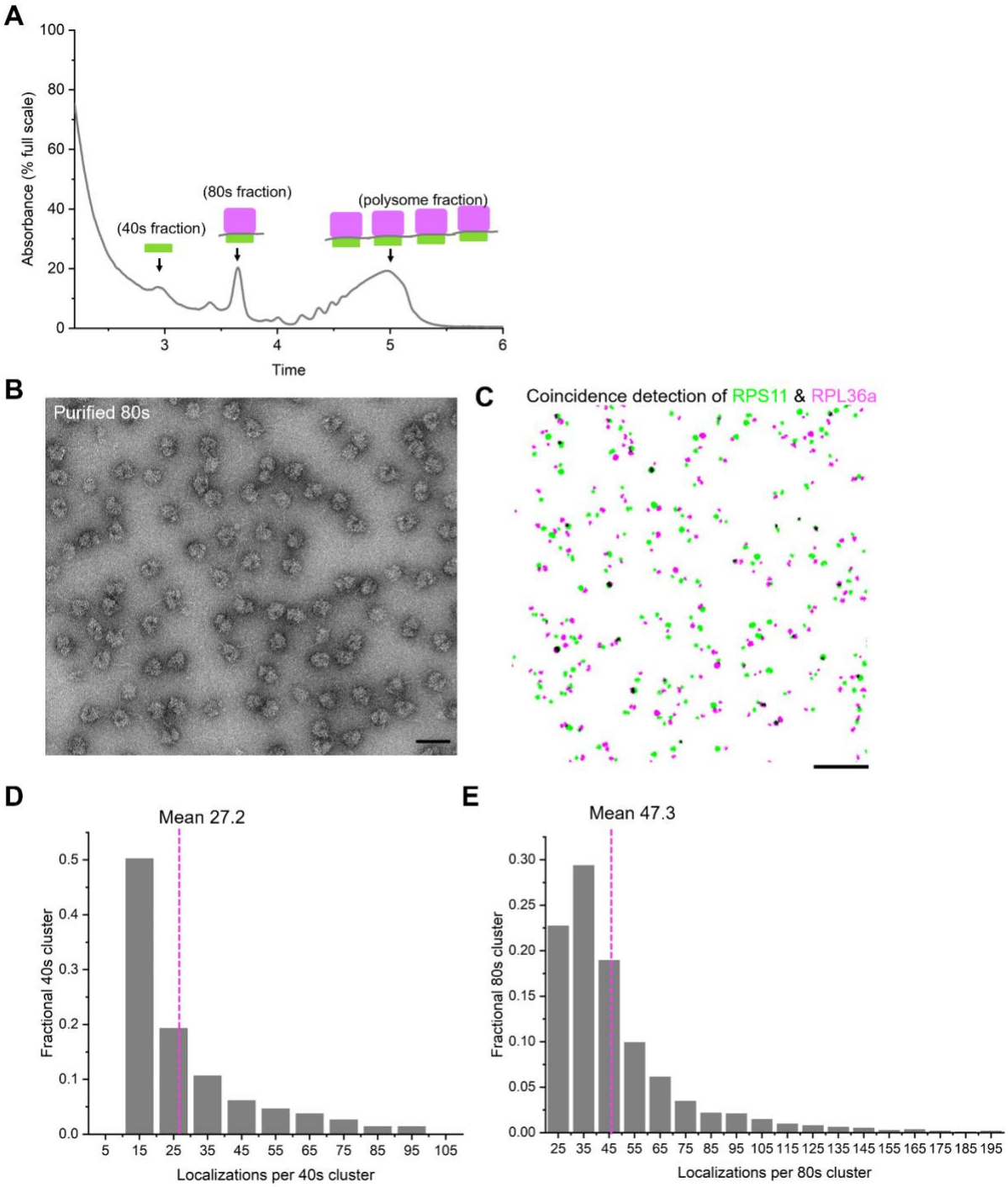
A
Absorbance (% full scale)
Time
(40s fraction)
(80s fraction)
(polysome fraction)
B
Purified 80s
C
Coincidence detection of RPS11 & RPL36a
D
Mean 27.2
Fractional 40s cluster
Localizations per 40s cluster
E
Mean 47.3
Fractional 80s cluster
Localizations per 80s cluster

Fig. S2.

Quantitative, multiplexed, single-molecule localization of assembled ribosomes (A) Representative polysome profile of the cultured rat neuronal lysate (18-21 DIV). Ribosomal small-subunit fraction (40s), 80s fraction, and polyribosome fraction are indicated and illustrated by respective cartoons. **(B)** Transmission electron micrograph of purified 80s ribosomes with negative staining. Scale bar: 50nm. **(C)** Co-localization between ribosomal large-(magenta) and small-(green) subunits from DNA PAINT of purified ribosomes plated on poly-lysine coated Mettek dishes. Scale bar: 500nm. **(D)** Distribution of small-subunit clusters in enriched 40s fractions from polysome profiling of lysates of cultured neurons. The average 40s cluster size was 27.2 localizations. **(E)** Distribution of colocalization clusters in enriched 80s fractions from polysome profiling of lysates of cultured neurons. The average colocalization-cluster size was 47.3 localizations.

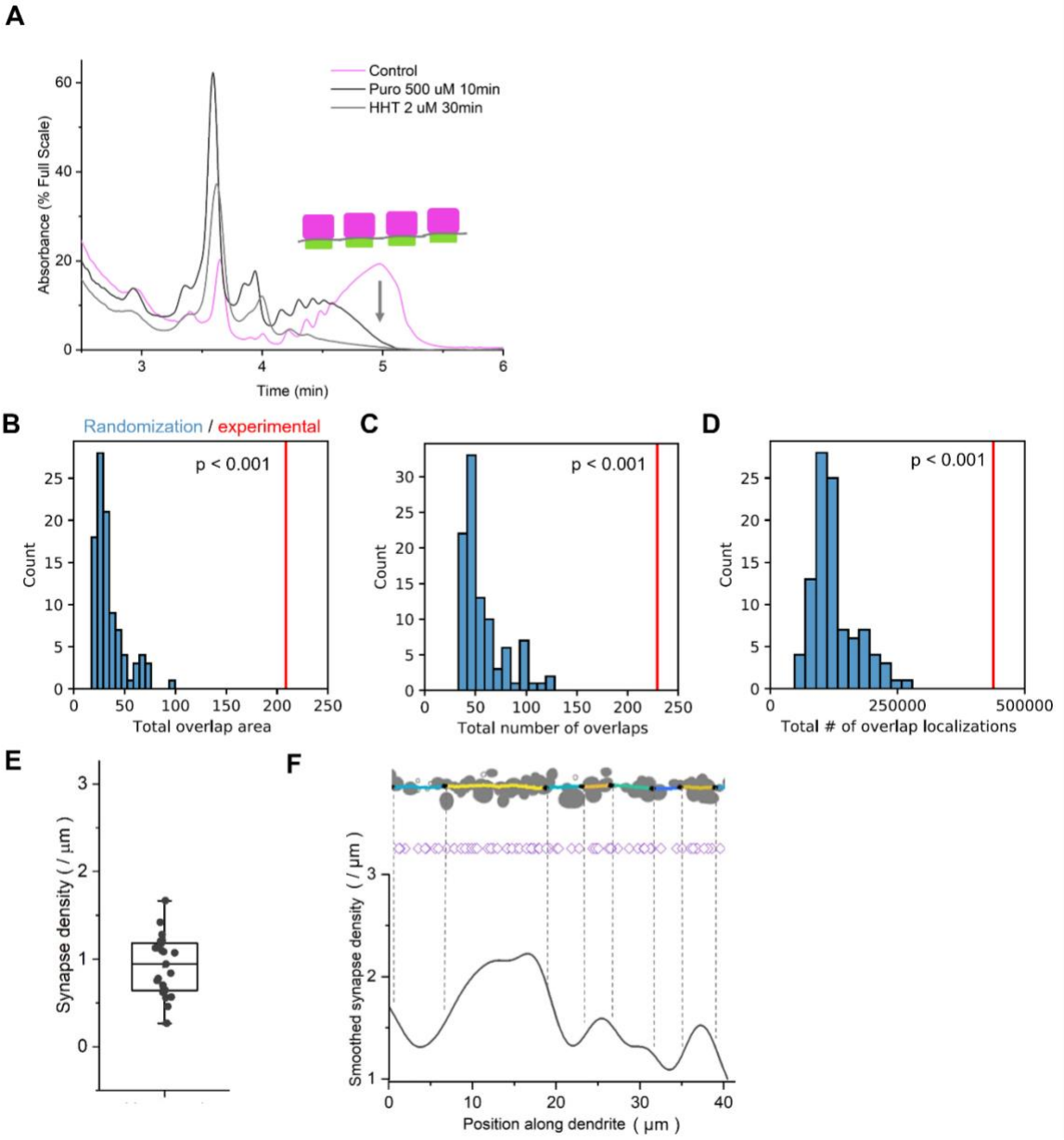
A
Control
Puro 500 uM 10min
HHT 2 uM 30min
Absorbance (% Full Scale)
Time (min)
B
Randomization / experimental
p < 0.001
Count
Total overlap area
C
p < 0.001
Count
Total number of overlaps
D
p < 0.001
Count
Total # of overlap localizations
E
Synapse density (/ µm)
F
Smoothed synapse density (/ µm)
Position along dendrite (µm)

Fig. S3.

Single-molecule localization of assembled ribosomes in neuronal dendrites. (A) Polysome profiles of cultured neurons treated with puromycin (Puro, 500 μM, 10 min; grey), homoharringtonine (HHT, 2 μM, 30 min; lighter grey), or untreated (control; magenta). There was a significant loss of polyribosomes upon treatment with either Puro or HHT (indicated by grey arrow). **(B)-(D)** Degree of colocalization between small- and large- subunits (characterized by overlap area, frequency, and localizations) for randomized cluster distribution (blue histogram) and experimental data (red line). Simulations indicate that experimental co-localization lies outside the probability distribution of random ($p < 0.001$). **(E)** Column scatter plot showing the synapse densities of cultured rat hippocampal neurons (DIV 18-21; 23 dendritic branches from 6 cell replicates). **(F)** Dendrites were segmented based on the heterogeneity of synapse density (y-axis) along dendrites (x-axis). The peaks and valleys of the density fluctuation are identified. The turning points between peaks and valleys were identified as the borders between segments (see methods). The resulting division matches the visible changes in synapse density (top cartoon) in a synapse; dendritic shafts are colored and segmented by boundaries depicted by black dots). Pink hollow spades below represent the positions of synapses along the dendritic length.

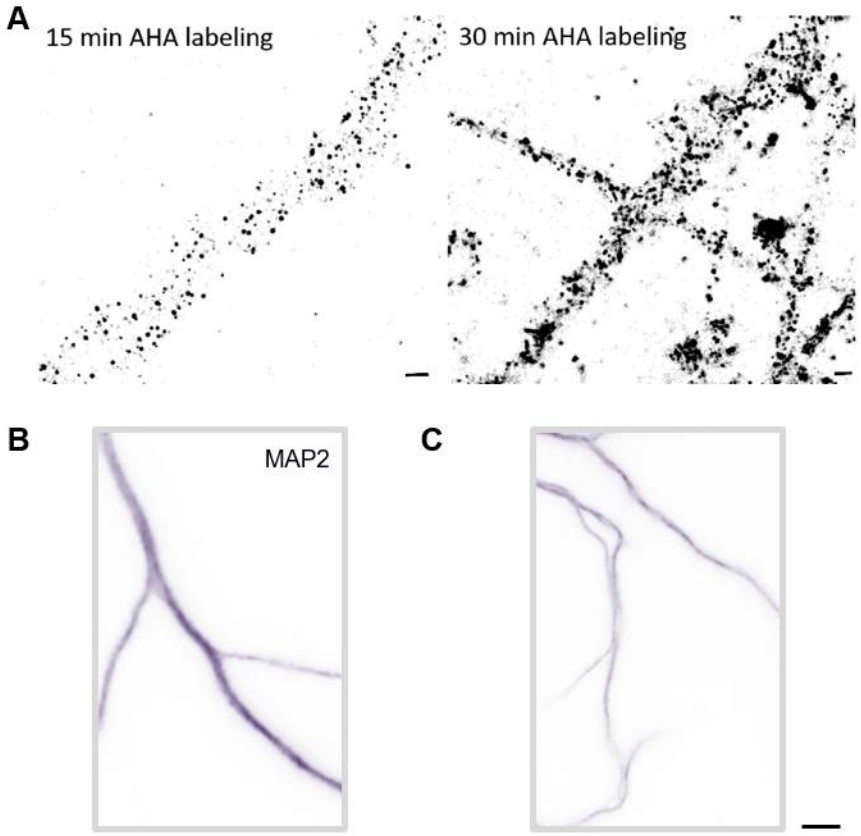
A
15 min AHA labeling
30 min AHA labeling
B
MAP2
C

Fig. S4.

DNA-PAINT images showing localizations of nascent proteins after different AHA labeling periods. (A) Left: after a 15 min AHA labeling, as used in this study. Right: after a 30 min AHA labeling showing crowding and merging of signal clusters, compromising quantitative analyses. Scale bars: 0.5 µm. **(B)** and **(C)** shows the corresponding anti-MAP2 immunolabelling for the regions of interest in Fig. 2B and 2C in the main text. Scale bar = 6 µm.

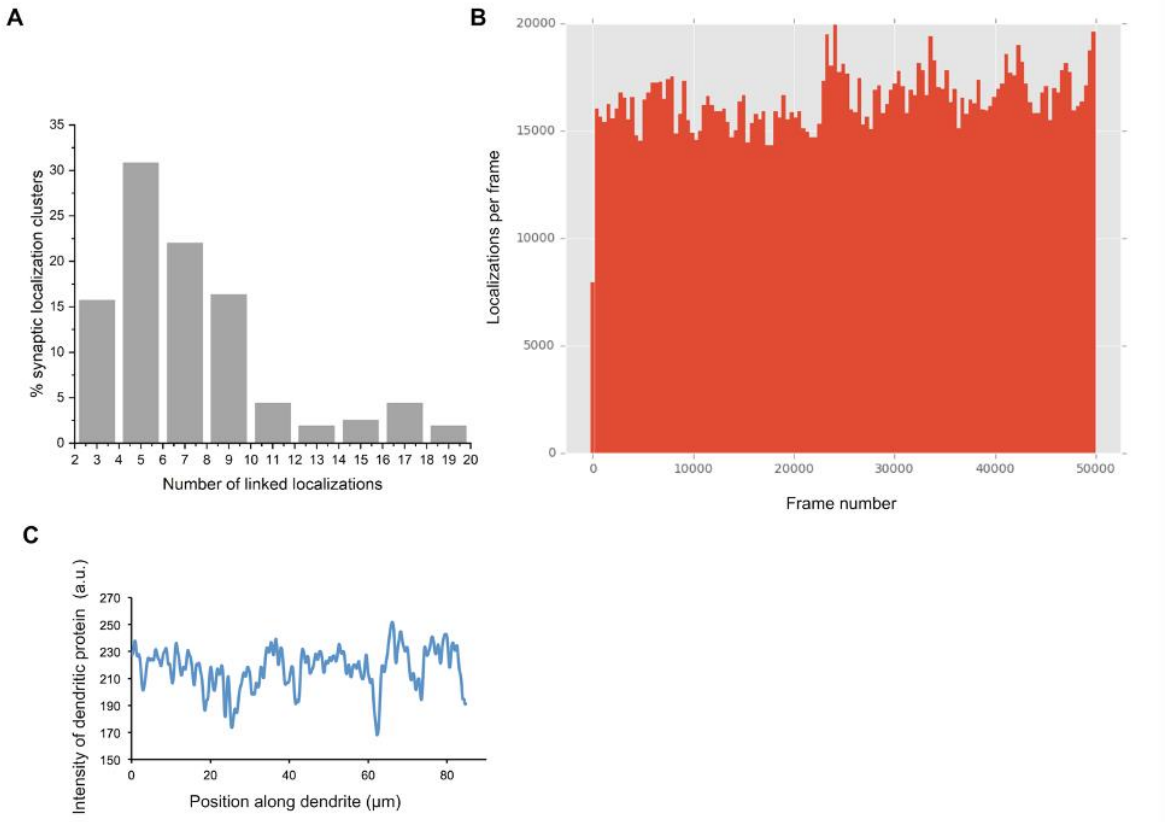
A
% synaptic localization clusters
Number of linked localizations
B
Localizations per frame
Frame number
C
Intensity of dendritic protein (a.u.)
Position along dendrite (µm)

Fig. S5.

Characterization of DNA PAINT nascent protein clusters. (A) Distribution of nascent-protein localization clusters at individual synapses. We designated the smallest population of clusters (bins between 3 and 11 linked localizations; bin size: 2) as one protein copy carrying a single docking oligo (Boeger et al, 2019). The average dark time ($\tau_{dark,\ single} \sim 1349$ s) is estimated for a single docking oligo. The larger-cluster population (e.g. 16-18 localization bins) likely contains more than one docking oligo due to multiple copies of proteins (see methods). **(B)** Localization counts per frame showed no decrease over 50,000 frames, indicating negligible bleaching. **(C)** Line graph showing the local fluctuations in tagged dendritic nascent-protein level approximated by the super-resolved image intensity (arbitrary units, a.u.) along a secondary dendritic branch (5-µm thick line profile).

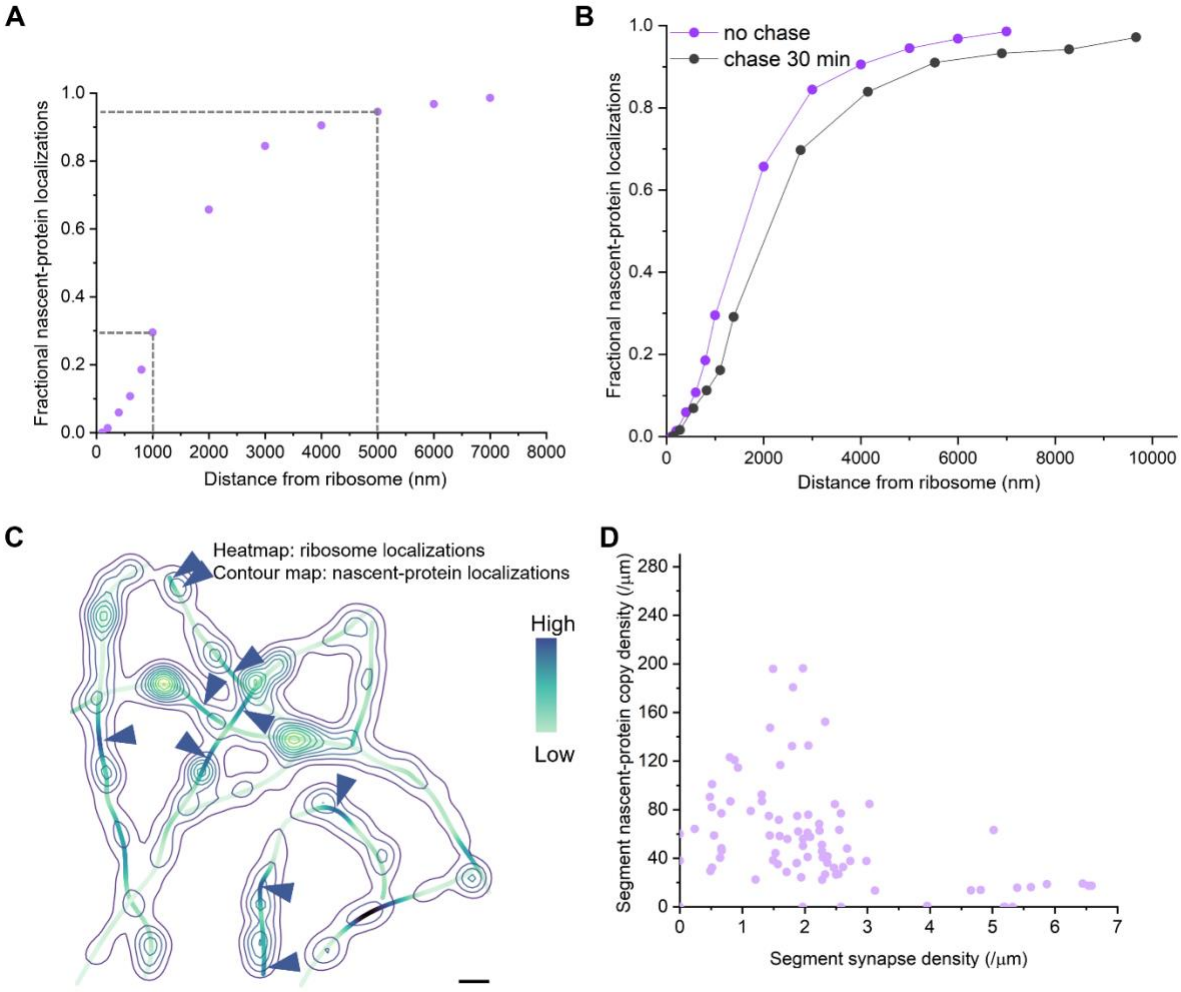
A
Fractional nascent-protein localizations
Distance from ribosome (nm)
B
no chase
chase 30 min
Fractional nascent-protein localizations
Distance from ribosome (nm)
C
Heatmap: ribosome localizations
Contour map: nascent-protein localizations
High
Low
D
Segment nascent-protein copy density (/μm)
Segment synapse density (/μm)

Fig. S6.

The spatial relationship between tagged nascent-protein cohorts and local sites of protein synthesis. (A) A cumulative plot showing the fraction of nascent-protein localizations (y axis) in relation to their spatial vicinity to nearby sites of mRNA translation (ribosomes; x axis). Dashed lines indicate ~30% of nascent proteins were within a 1 μm radius of at least one ribosome and that over 90% nascent proteins were within a 5 μm radius of at least one ribosome. **(B)** Cumulative distribution plots showing the fraction of nascent-protein localizations (y axis) in relation to their spatial proximity to nearby sites of translation (ribosomes; x axis) with (black) and without a 30 min chase (purple) following metabolic labeling. **(C)** Representative view (4300 μm^2) of the distribution of nascent-protein localizations (contour map) and ribosome localizations (heatmap) in the dendritic arbor when a 30 min chase was imposed following metabolic labeling. Lighter green contours represent local hotspots of nascent-protein localizations. Top right legend shows the color scheme for the synapse-density heatmap. Blue filled triangles indicate the local hotspots of ribosomes displaced from the local nascent-protein maxima (peaks of contour map. Scale bar: 5 μm. **(D)** Scatter plot showing the absence of positive correlations between nascent-protein density (y axis; localization density) and synapse density (x axis) following 30min chase, indicating that nascent proteins have diffused from where ribosomes congregate to translate.

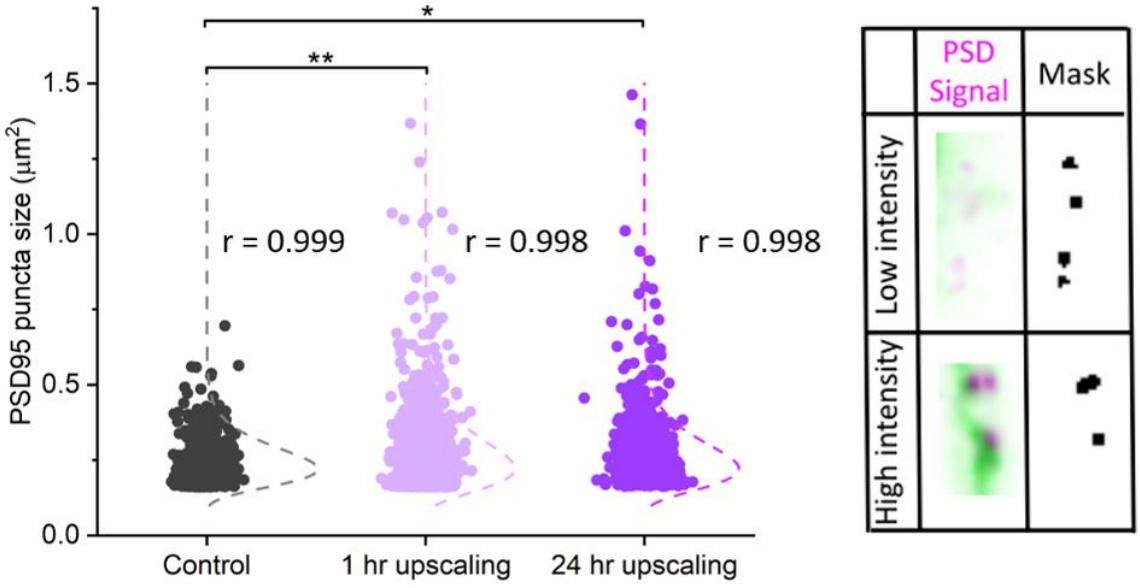
*
**
1.5
1.0
0.5
0.0
PSD95 puncta size (μm²)
r = 0.999
r = 0.998
r = 0.998
Control
1 hr upscaling
24 hr upscaling
PSD Signal
Mask
Low intensity
High intensity

Fig. S7.

Characterization of PSD95 puncta size. Scatter plots indicating the measured PSD puncta size distribution for the synapses belonging to the dendrites in untreated (black, 371 puncta) neurons, and neurons in the upscaling 1 hr (lavender, 766 puncta), and upscaling 24 hr (purple, 906 puncta) conditions. There were significant differences between control and the upscaling groups (ANOVA with Bonferroni post hoc analysis; p*<0.05, p**<0.01). r values indicate goodness-of-fit to a log-normal distribution (indicated by dashed lines). Right inset show examples of diffraction-limited PSD95 puncta and their corresponding identifications by local thresholding, regardless of local intensity differences.

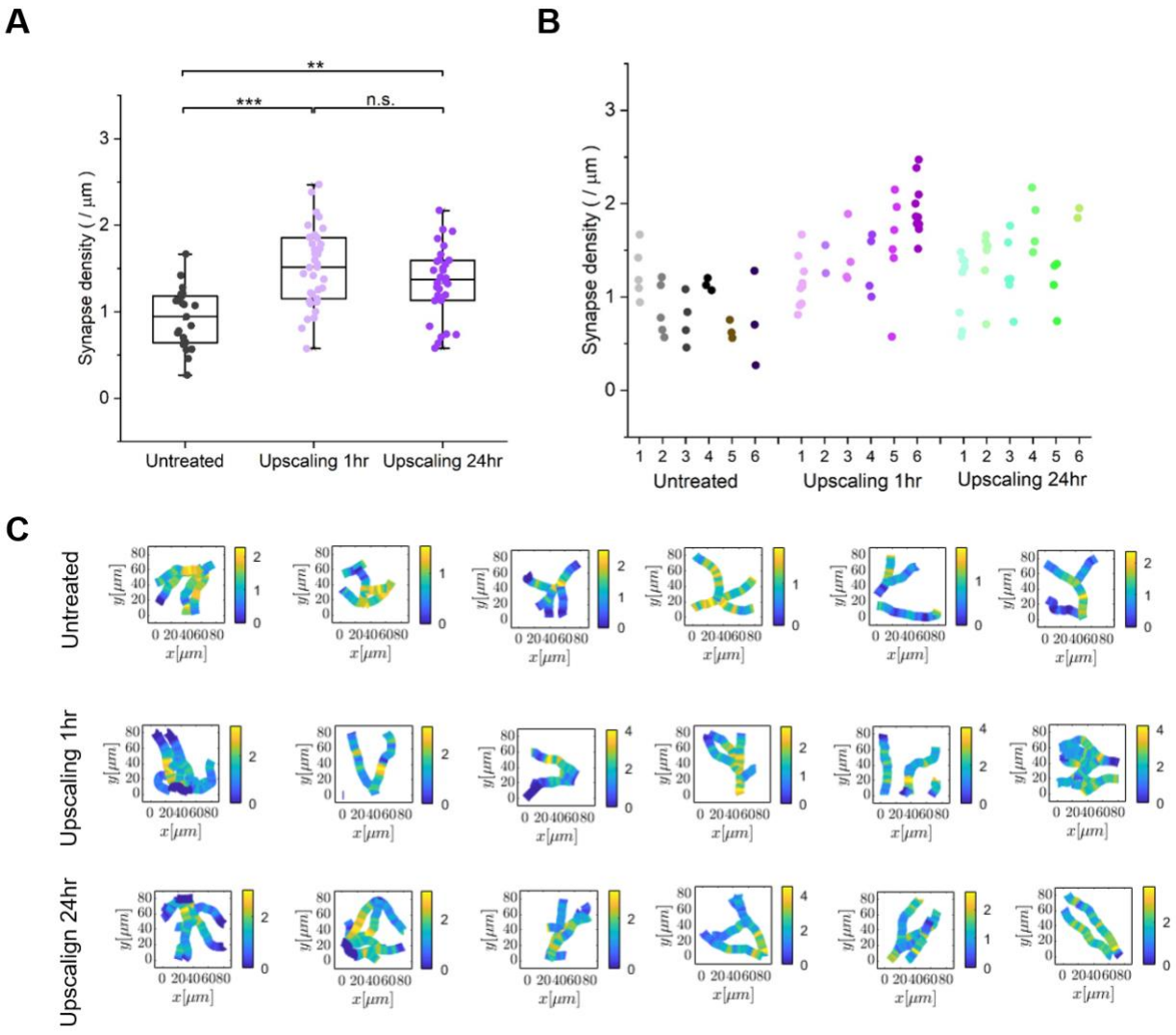
A
B
C
**
***
n.s.
Synapse density (/ µm)
Untreated
Upscaling 1hr
Upscaling 24hr
Upscalign 24hr
x[µm]
y[µm]

Fig. S8.

Synapse density of all dendritic branches. (A) Scatter plots indicating the synapse densities (per µm dendritic length) for 23 dendritic branches from 6 untreated cells (grey), 34 branches from 6 cells treated with 2 µM TTX for 1 hr (lavender), 29 branches from 6 cells treated with 2 µM TTX for 24 hr (purple). ANOVA with Bonferroni post hoc analysis indicated a significant increase in synapse density after both 1 hr ($p < 0.001$) and 24 hr ($p < 0.01$) upscaling, and no significant difference between 1 hr and 24 hr upscaling (*$p<0.05$; **$p<0.01$; ***$p<0.001$). The same description applies for all following box plots unless otherwise noted. **(B)** Column scatter plots of synapse density from all dendritic branches in all cell replicates (each column corresponds to the dendritic branches from a single neuronal replicate). **(C)** Heatmaps showing synapse distribution in all the dendritic branches.

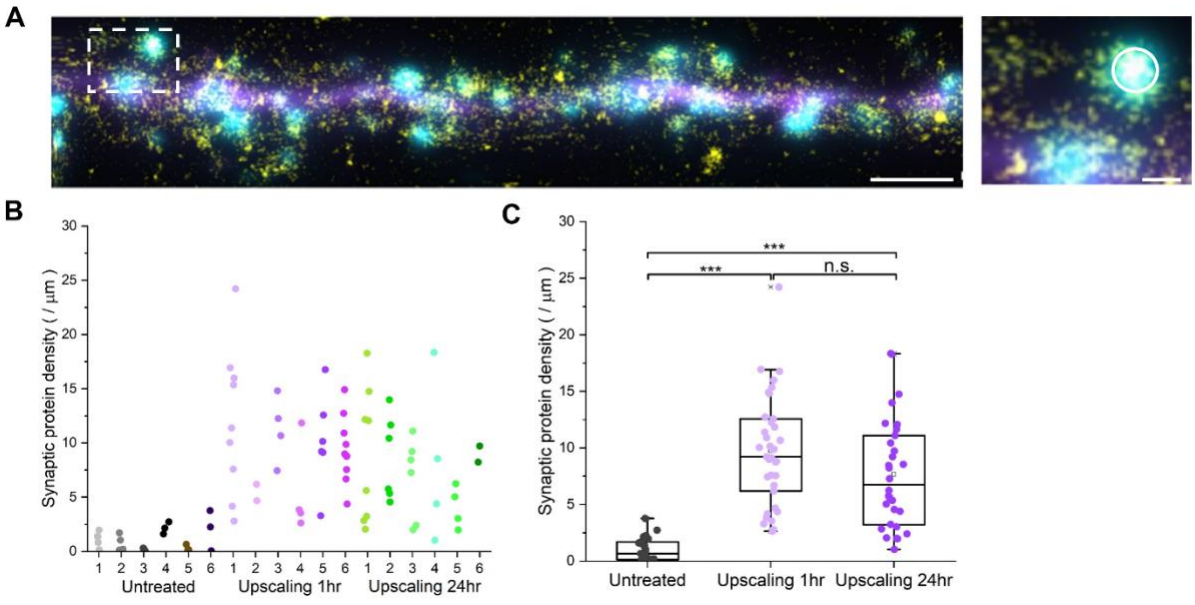
A
B
C
Synaptic protein density (/ µm)
Untreated
Upscaling 1hr
Upscaling 24hr
***
***
n.s.

Fig. S9.

Nascent proteins in dendrites under basal conditions and after scaling. **(A)** A representative straightened dendritic branch with its nascent-protein localizations (magenta: anti-MAP2 immunolabel; cyan: anti-PSD95 immunolabel; yellow: all linked protein localizations without cluster identification). Total dendritic protein localizations include localizations that are within 2.5 µm from the center line of branch (see methods). Scale bar: 2.5 µm. The white dashed box indicates the region corresponding to the right inset. Right inset: localizations in an example synapse (circled area). Scale bar: 0.5 µm. **(B)** Column scatter plots of synaptic protein (localizations; locally synthesized, nascent) densities from all dendritic branches in all cell replicates (each column corresponds to the dendritic branches of a neuron replicate). **(C)** Column scatter plots of synaptic protein (localizations; locally synthesized, nascent) density per unit dendritic length. There were significant increases in synaptic protein density after both 1 hr ($p<0.001$) and 24 hr ($p<0.001$) upscaling (ANOVA with Bonferroni post hoc analysis; *$p<0.05$; **$p<0.01$; ***$p<0.001$).

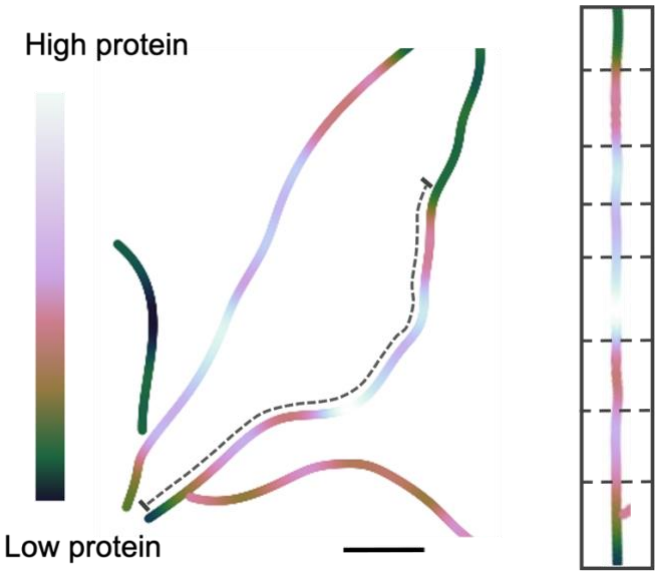
High protein
Low protein

Fig. S10.

Heatmap of synaptic nascent-protein density In a representative dendrite (cell soma located in the bottom-left direction of the graph), the density map exhibited spatial heterogeneity at an intermediate length-scale (10^0 - 10^1 μm). Scale bar: 10 μm. Right inset box illustrates the emergence of local domains with high and low densities of synaptic proteins.

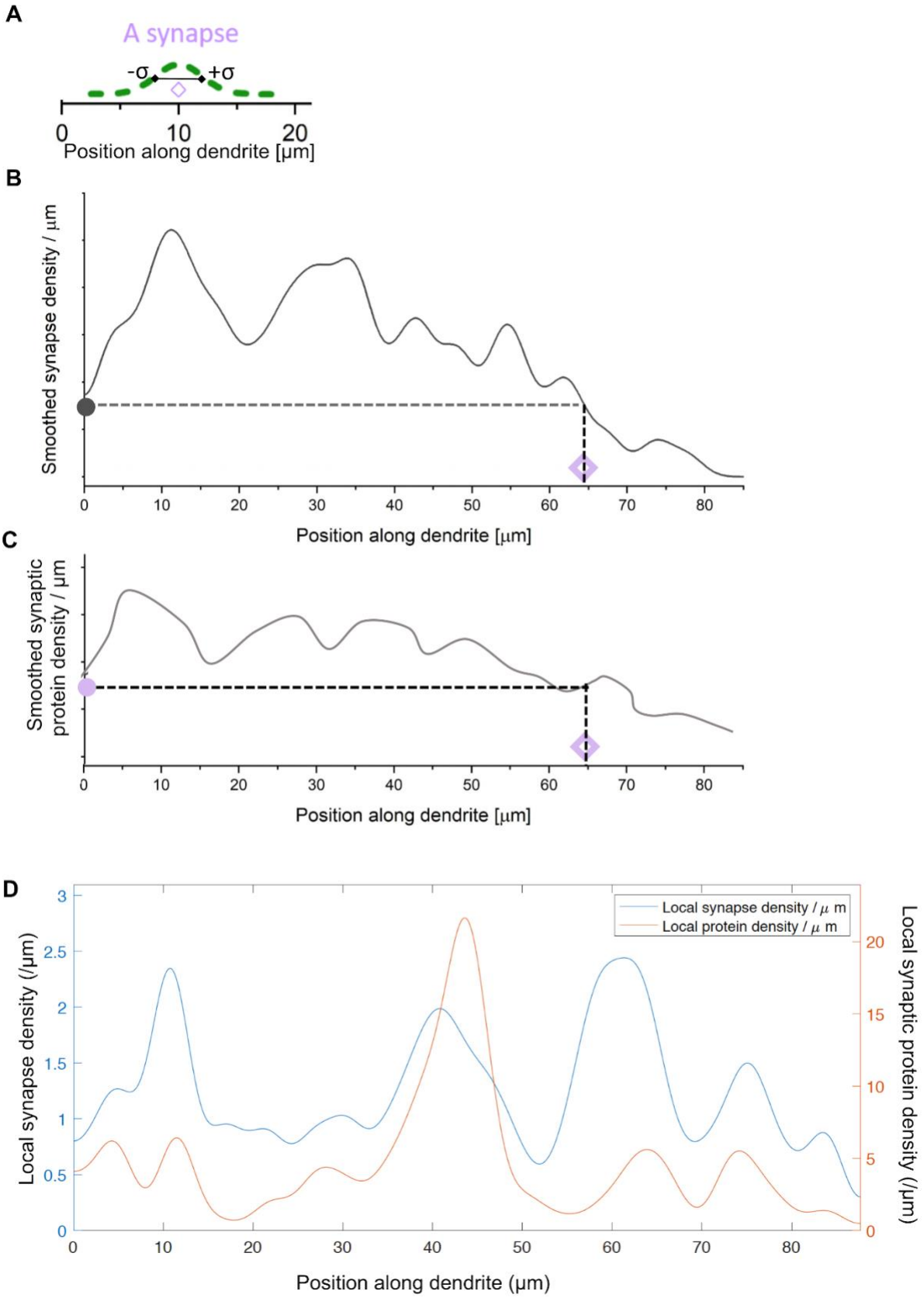
A
A synapse
-σ
+σ
0
10
20
Position along dendrite [μm]
B
Smoothed synapse density / μm
0
10
20
30
40
50
60
70
80
Position along dendrite [μm]
C
Smoothed synaptic protein density / μm
0
10
20
30
40
50
60
70
80
Position along dendrite [μm]
D
Local synapse density / μ m
Local protein density / μ m
Local synapse density (/μm)
Local synaptic protein density (/μm)
0
0.5
1
1.5
2
2.5
3
0
5
10
15
20
0
10
20
30
40
50
60
70
80
Position along dendrite (μm)

Fig. S11.

Density fluctuations of synapses and synaptic nascent-protein density. (A) Every synapse's contribution to synapse density is approximated as a unit Gaussian with a standard deviation, σ = 2 µm. X axis indicates the position of a synapse along the dendrite. **(B)** The fluctuation of synapse density (Y axis) along a dendritic branch (X axis) generated from the superposition of all synapse Gaussians. Knowing a synapse's location on a dendrite (e.g. hollow pink diamond), one can measure the local synapse density (black dot on the Y axis). **(C)** The fluctuation of synaptic protein (locally synthesized, nascent) density (Y axis) along a dendritic branch (X axis) generated from the superposition of all synapse Gaussians using a similar method described in B, with each synapse's contribution proportional to its protein allocation level. Knowing a synapse's location on a dendrite (e.g. hollow pink diamond), one can measure the local synaptic protein density (pink dot on the Y axis). **(D)** Fluctuations of synapse density and synaptic protein (locally synthesized, nascent) density along an example dendritic branch from the 1 hr upscaling group. Notice the lack of general increase of synaptic protein density with increasing proximity-to-the-soma (towards position 0 on x axis), consistent with Fig. S5C and a local nascent protein source.

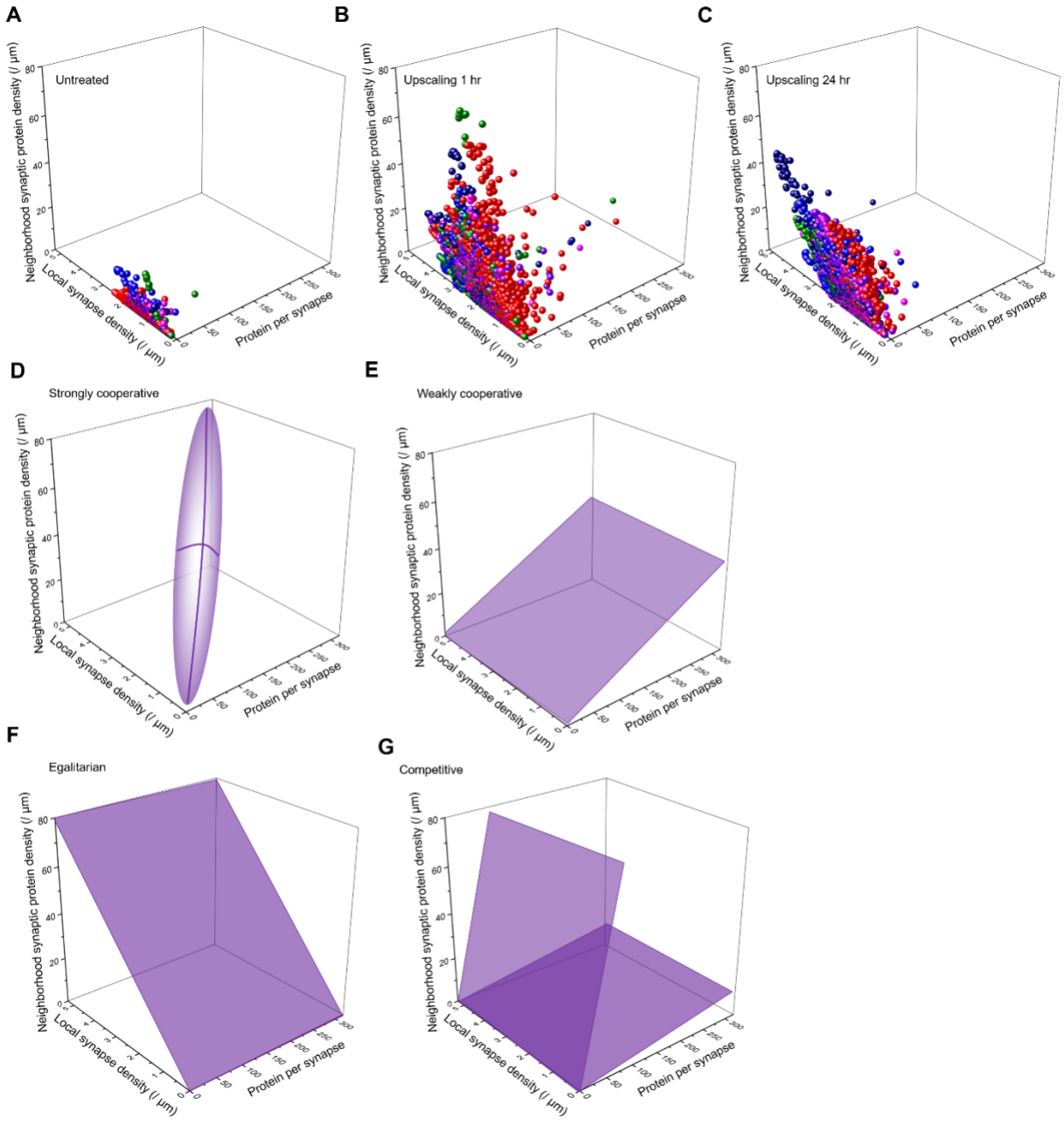
A
Untreated
B
Upscaling 1 hr
C
Upscaling 24 hr
D
Strongly cooperative
E
Weakly cooperative
F
Egalitarian
G
Competitive
Neighborhood synaptic protein density (/ µm)
Local synapse density (/ µm)
Protein per synapse

Fig. S12.

The contribution of local protein supply to the synapse population following upscaling. (A)-(C) 3D scatter plots of 1289 synapses from 6 untreated neurons (synapses from each neuron share the same color) (A); 2955 synapse from 6 upscaling 1 hr neurons (B); and 2625 synapses from 6 upscaling 24 hr neurons (C). X axis: Local synapse density; Y axis: protein (localizations; locally synthesized, nascent) per synapse; Z axis: Local synaptic protein (localizations; locally synthesized, nascent) density. **(D)-(G)** Schemes showing the different types of synaptic protein-supply distribution in the parameter space defined in A, B and C. For example, B resembles G (competitive) while A resemble E (weakly cooperative).

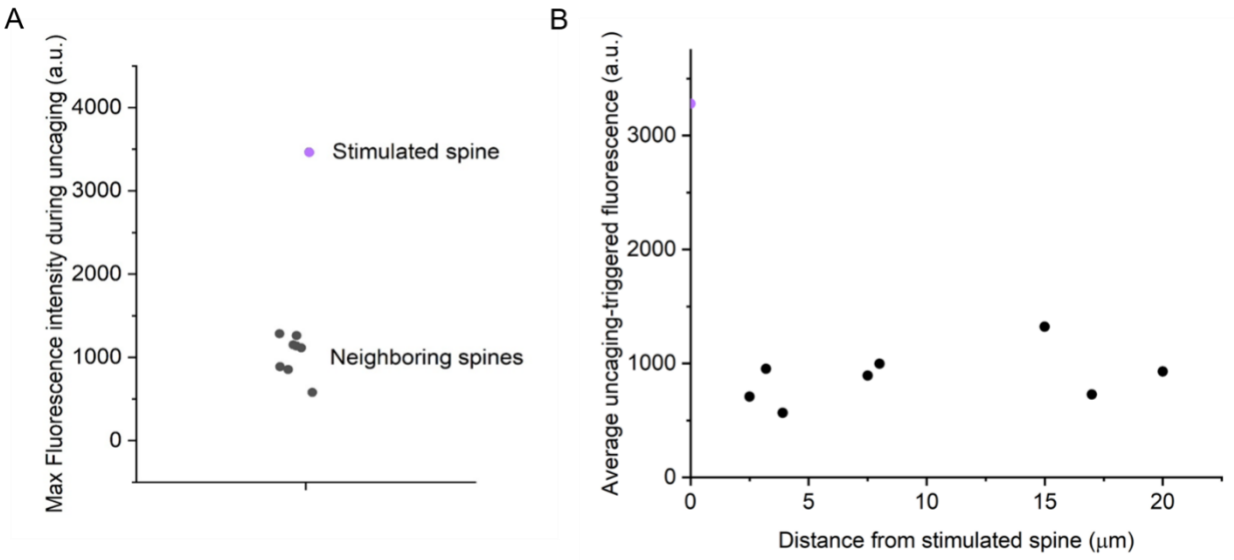
A
Max Fluorescence intensity during uncaging (a.u.)
4000
3000
2000
1000
0
Stimulated spine
Neighboring spines
B
Average uncaging-triggered fluorescence (a.u.)
3000
2000
1000
0
0
5
10
15
20
Distance from stimulated spine (μm)

Fig. S13.

The specificity of uncaged glutamate induced spine Ca^{2+} response. (A) Scatter plot showing the maximum GCaMP6s fluorescence (indicating Ca^{2+} level) detected during glutamate uncaging for a representative target spine (magenta) and its neighboring spines (grey; residing as far as 20 µm away). (B) Scatter plot showing average glutamate-uncaging triggered Ca^{2+} levels of neighboring spines in relation to their distances from the stimulated spine. The magenta datapoint (at x = 0) indicates the target spine. Black datapoints indicate neighboring spines.

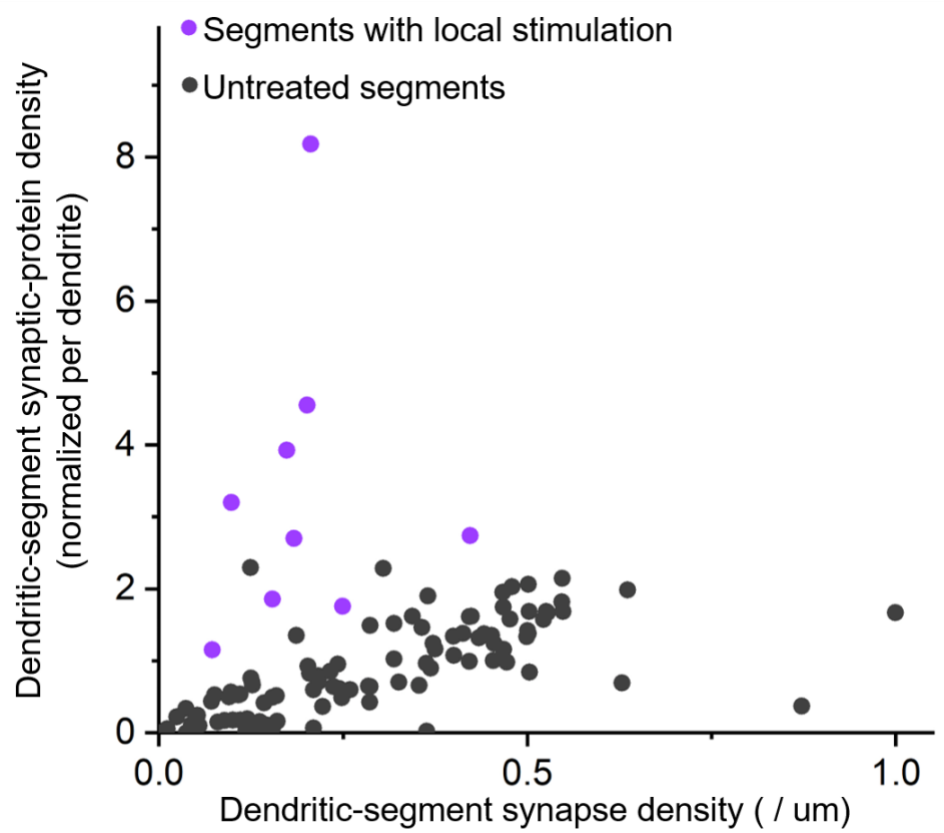
Segments with local stimulation
Untreated segments
Dendritic-segment synaptic-protein density
(normalized per dendrite)
0
2
4
6
8
0.0
0.5
1.0
Dendritic-segment synapse density (/ um)

Fig. S14.

Dendritic segments containing stimulated spines exhibited elevated nascent-protein levels. Scatter plot showing the correlations between normalized synaptic-protein density (Y) and synapse density (X) for 128 dendritic segments including 9 segments with stimulated spines (magenta) and 119 control segments without local stimulation (dark grey). Neighboring dendritic segments (subsets of dark grey dots) did not show significant differences from other control segments.